



Microwave ablation combined with immune checkpoint inhibitor enhanced the antitumor immune activation and memory in rechallenged tumor mouse model

Fengkuo Xu¹ · Jing Sang² · Nan Wang³ · Meixiang Wang¹ · Yahan Huang⁴ · Ji Ma¹ · Huanan Chen^{1,5,6} · Qi Xie^{1,7} · Zhigang Wei^{1,8} · Xin Ye^{1,7} 

Received: 29 December 2024 / Accepted: 26 February 2025 / Published online: 25 March 2025
© The Author(s) 2025

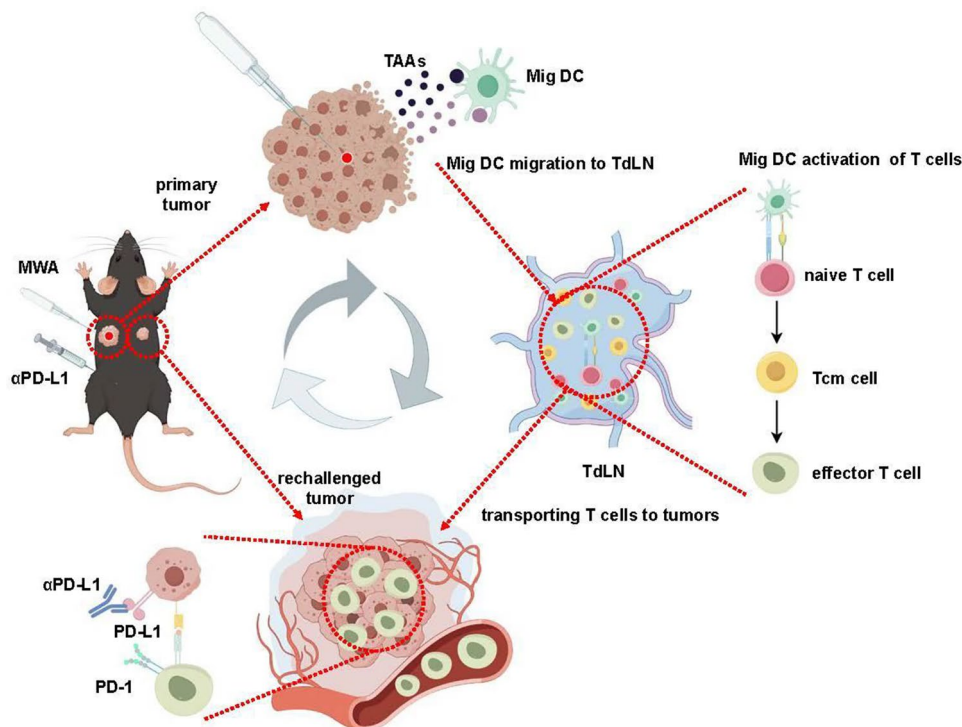
Abstract

Microwave ablation (MWA) is a super minimally invasive therapeutic approach that has been widely applied in the treatment of non-small cell lung cancer (NSCLC). Although MWA can elicit antitumor immune responses, these immune responses are not relatively steady and insufficient to completely clear recurrence tumor cells within the body. Immunotherapy monotherapy has shown low clinical efficacy in the treatment of advanced NSCLC. MWA combined with immune checkpoint inhibitors (ICIs) is a promising therapeutic approach. However, the mechanism of synergic effect remains elusive. In this study, we have conducted a retrospective analysis of the clinical outcomes of MWA combined with ICIs, finding that the combinational therapy yielded superior Objective Response Rate and longer Progression-Free Survival. In preclinical models, we established a tumor rechallenged model to address post-MWA recurrence and to delve into the underlying mechanisms of the combined therapy. We observed that the combined treatment (MWA + PD-L1 blockade therapy) effectively addressed the issue of tumor recurrence in tumor rechallenged model. The combinational therapy increased the function and percentage of CD8⁺ tumor-infiltrating lymphocytes, enhanced the functionality of CD8⁺ T cells within tumor-draining lymph nodes (TdLNs), and elevated the proportion of T central memory cells. Additionally, the combined treatments promoted the proportion of Migration Dendritic Cells type 1 (Mig DC1) within TdLNs, thereby enhancing their activation potential. Notably, FTY720-mediated blockade of lymphocyte egress abolished the therapeutic benefits, confirming TdLNs-dependent systemic immunity. Moreover, the efficacy of the combinational therapy depended on the migration of T cells from TdLNs to tumor site. In summary, we proposed a potentially effective combined treatment regimen and have elucidated the underlying cellular mechanisms that underpin its efficacy.

Fengkuo Xu, Jing Sang and Nan Wang have contributed equally to this article and should be considered co-first authors.

Extended author information available on the last page of the article

Graphical abstract



After microwave ablation (MWA) of the primary tumor, the release of tumor-associated antigens (TAAs) occurs. These antigens are then internalized by Migration-Directed Dendritic Cells type 1 (Mig DC1), which subsequently migrate to the tumor-draining lymph nodes (TdLNs). Within the microenvironment of the TdLNs, Mig DC1 presents these antigens to naive T cells, prompting their differentiation into T central memory (Tcm) cells. In the context of the combined therapeutic approach, which includes MWA and PD-L1 blockade therapy, a greater number of Tcm cells are induced and activated, allowing for a rapid response to tumor re-challenge. These Tcm cells differentiate into effector T cells and migrate to the tumor site to exhibit antitumor activity.

Keywords Microwave ablation · Immune checkpoint inhibitors · PD-L1 · CD8⁺T cells · Dendritic cells

Introduction

The latest statistics data reveals that lung cancer stands with the highest rates of incidence and cancer-related deaths, highlighting the urgent need for improved diagnosis and treatment strategies [1]. Image-guided thermal ablation (IGTA), as a super minimally invasive treatment modality, has matured in its application for primary lung tumors [2]. The common ablation methods include radiofrequency ablation (RFA), microwave ablation (MWA), and cryoablation [3]. MWA is particularly advantageous in the treatment of lung tumors due to its larger ablation zone, shorter ablation time, and lower sink heat effect [4]. Additionally, MWA can induce local coagulative necrosis and the release of tumor

antigens, including tumor-associated antigens (TAAs), heat shock proteins (HSPs) and damage associated molecular patterns (DAMPs), at the tumor site [5–7]. This process recruits dendritic cells (DC), natural killer (NK) cells, and T cells, thereby activating antitumor immunity and possibly eliciting an abscopal effect in some cases [8]. However, the antitumor immune response induced by MWA is unstable and cannot effectively suppress tumor growth in the long term, leading to the post-MWA recurrence. This limitation restricts the clinical treatment effect [9].

Immunotherapy, exemplified by immune checkpoint inhibitors (ICIs), targeting cytotoxic T-lymphocyte antigen-4 (CTLA-4), programmed cell death protein 1 (PD-1), or programmed cell death protein ligand 1 (PD-L1), have

revolutionized the concept and practice of cancer treatment in recent years [10, 11]. This approach has achieved pioneering advancements in the field of lung cancer treatment, successfully prolonging the survival of certain patients [12, 13]. ICIs monotherapy showed low clinical efficacy in the treatment of advanced NSCLC [14].

An increasing number of studies are focusing on combination therapy approaches to improve treatment outcomes [15–18], among which the combination of MWA and ICIs is a promising treatment option. We retrospectively evaluated the efficacy of MWA combined with ICI in the treatment of advanced NSCLC. It found that the combination therapy demonstrated a higher Objective Response Rate (ORR) and longer Progression-Free Survival (PFS) compared to ICI monotherapy. Our results indicated that the combination treatment enhanced the clinical efficacy of ICI in advanced NSCLC. Preclinical studies are currently underway to explore the potential mechanisms of the combined therapy. MWA in conjunction with LAG3 blockade reprogrammed the tumor microenvironment (TME), significantly promoting the proliferation and function of CD8⁺ tumor-infiltrating lymphocytes (TILs) [19]. The combination of RFA with PD-1 inhibitor significantly enhanced antitumor T cell immune responses [20]. In clinical practices, ICIs combined with MWA improved the clinical efficacy. However, the mechanism of synergic effect remains elusive. Therefore, we employed a tumor rechallenged model, simulating the scenarios of advanced progression and tumor recurrence, to further elucidate the underlying mechanisms and address post-ablation recurrence. We observed that tumor recurring post-MWA exhibited upregulated PD-L1 expression. Subsequently, we explored the therapeutic synergy of MWA with anti-PD-L1 antibodies, aiming to broaden the indications for this combined modality. Our findings not only validated the clinical benefits of MWA-ICI combination but also shed light on its mechanistic basis, paving the way for expanded clinical applications.

Materials and methods

Patients

Sixty-two patients with NSCLC who underwent ICIs or ICIs combined with MWA at The First Affiliated Hospital of Shandong First Medical University were enrolled, from January 1, 2019 and January 1, 2022.

The inclusion criteria were as follows: (1) pathologically verified NSCLC; (2) advanced tumor stage, including stages IIIB and IV; (3) Eastern Cooperative Oncology Group performance status of 0–2; (4) at least one measurable tumor lesion after MWA procedure; (5) capable of tolerating combined therapy. (6) wild-type epidermal growth factor

receptor and anaplastic lymphoma kinase based on genetic test results.

The exclusion criteria were as follows: (1) history of other cancer within the preceding five-year period; (2) intolerant to ICIs; (3) other antitumor treatments performed during the observation period; (4) long-term hormone or antibiotic therapy. (5) Presence of moderate or severe interstitial pulmonary disease. (6) Those who were lost to follow-up. Approval for this retrospective study, which complied with the standards of the Declaration of Helsinki, was obtained from Institutional Ethics Committee of the institutions, and informed consent was waived due to the retrospective nature of this study. The baseline characteristics are listed in Table 1.

Treatment regimens

The equipment, basic materials, and care measures required for the MWA procedure were performed as described previously [15, 21, 22]. MWA procedure was conducted under percutaneous computed tomography (CT) guidance. KY-2450B (CANYOU Medical Inc., CFDA Certificated No.: 20153251727) microwave ablation system was applied for the procedure with a frequency of 2450 ± 50 MHz and an adjustable continuous wave output power of 0–100 W. For tumors with a maximum dimension ≤ 10 mm, ablation is typically performed by positioning a single 19-G (19-gauge) antenna at the tumor center. When targeting tumors measuring 10–30 mm in maximum dimension, a conformal ablation strategy utilizing double-antennas with multiple needle adjustments is routinely employed. The treatment regimen for these patients included MWA combination with camrelizumab (a PD-1 antibody designed by Hengrui Pharm, Jiangsu Province, China), as well as camrelizumab monotherapy. The selection of treatment strategies is formulated based on the individualized condition of the patient, multidisciplinary consultations, and the patient's own preferences. MWA combination with camrelizumab group: camrelizumab was administered 5–7 days after MWA, a 30-min intravenous infusion at a dose of 200 mg every 2 or 3 weeks until disease progression or unacceptable toxicity. Camrelizumab monotherapy group: camrelizumab was administered a 30-min intravenous infusion at a dose of 200 mg every 2 or 3 weeks until disease progression or unacceptable toxicity.

Assessments of clinical efficacy

All patients underwent a comprehensive clinical assessment every three months, conducted by experienced clinicians based on the results of enhanced computed tomography scan or positron emission tomography—CT. The therapeutic analysis, encompassing complete response (CR), partial response (PR), stable disease (SD), and

Table 1 Baseline and treatment characteristics of enrolled patients

Characteristics	ICI (N = 30)	MWA + ICI (N = 32)	<i>p</i>
Gender, n (%)			0.4267
Male	28 (93.3)	27 (84.4)	
Female	2 (6.7)	5 (15.6)	
Age, year			0.8534
Median	66	67	
Range	38–85	57–78	
Smoking history, n (%)			0.7848
Nonsmokers	10 (33.3)	9 (28.1)	
Smokers	20 (66.7)	23 (71.9)	
ECOG, n (%)			0.9999
0	3 (10.0)	4 (12.5)	
1 or 2	27 (90.0)	28 (87.5)	
Pathology, n (%)			0.2169
Adenocarcinoma	12 (40.0)	18 (56.3)	
Squamous cell lung cancer	18 (60.0)	14 (43.7)	
Lymph nodes metastases, n (%)			0.4508
No	6 (20.0)	7 (21.9)	
Yes	24 (80.0)	25 (78.1)	
Stage, n (%)			0.6155
IIIB	16 (53.3)	14 (43.8)	
IV	14 (46.7)	18 (56.2)	
PD-L1 positive, n (%)			0.4950
< 1%	6 (20.0)	5 (15.6)	
≥ 1%, < 50%	8 (26.7)	9 (28.1)	
≥ 50%	4 (13.3)	4 (12.5)	
Unknown	12 (40.0)	14 (43.8)	

*Except where indicated, data are number (%). The Chi-square or Fisher exact test was applied for categorical variables. **Data were continuous variables, expressed in average ± standard deviation (range), and were compared using the Mann–Whitney *U* test. ICIs, Immune checkpoint inhibitors; MWA, microwave ablation; ECOG PS, Eastern Cooperative Oncology Group performance status

progressive disease (PD), were assessed with the Response Evaluation Criteria in Solid Tumors version 1.1 and subsequently compared across the two study groups.

Mice

C57BL/6 mice (6–8 weeks old) were purchased from Beijing Huafukang Biotechnology Co., LTD. (Beijing, China) and housed in a the specific-pathogen-free (SPF) facility at Shandong First Medical University & Shandong Academy of Medical Sciences (Shandong, China). All animal experiments were conducted according to protocols approved by the animal ethics committee of the Shandong First Medical University & Shandong Academy of Medical Sciences.

Cell lines

Lewis lung carcinoma cell line (LLC) was purchased from FuHeng Biology (Shanghai, China). All cell lines were grown in complete DMEM-10 medium: DMEM (Gibco, NY, USA), which consists of 10% (v/v) fetal bovine serum (FBS, Gibco, NY, USA), 100 U/mL penicillin, and 100 mg/mL streptomycin.

Tumor rechallenge model and treatment

LLC cells (5×10^5 cells/mouse) were injected subcutaneously into the right axillary fossa of mice on day 0. Upon reaching a tumor diameter of approximately 8–10 mm, mice were subjected to various therapeutic interventions around

day 8: no treatment, MWA alone, α PD-L1 antibody therapy alone, or a combination of MWA and α PD-L1 antibody. MWA was specifically performed on the tumor in the right axillary fossa on day 8, involving percutaneous insertion of an ablation electrode to the deepest extent of the tumor along its longitudinal axis. The procedure consisted of a 1.5-min treatment duration at a power output of 3 watts. For α PD-L1 antibody (10F.9G2, BioXcell, New Hampshire, USA) was administered at a dose of 200 μ g per mouse, beginning from day D1, with injections every 3 days, for a total of four doses. For FTY720 (HY-12005, MedChemExpress, China) injection, 2 mg/kg FTY720 dissolved in the 0.9% saline was injected intraperitoneally from Day-2 to Day10. For tumor rechallenge, LLC cells (2×10^6 cells/mouse) were injected subcutaneously into the left axillary fossa on day 9. Tumor growth in the left axillary fossa (abscopal site) was monitored every two days.

Mice ablation procedures

The animal ablation system is analogous to that used in patients, designed to achieve complete tumor ablation [23]. Mice were anesthetized using a animal anesthesia machine (R500, RWD) equipped with 3%–4% isoflurane and maintained under full anesthesia. Subsequently, a microwave ablation device (KY-2000, Kangyou) and a microwave ablation antenna (KY-2450A-6, Kangyou) were employed with ablation parameters set at 3 watts for 1 min.

CD8⁺ T cells depletion

Mice were treated with an initial intraperitoneal injection of 200 μ g/mouse of anti-CD8 antibodies (clone 2.43, BioXCell, NH, USA) dissolved in PBS, two days before the start of MWA treatments. This was followed by a maintenance dose of 100 μ g/mouse, administered every 4 days throughout the course of tumor growth. The control group received equivalent injections of control IgG.

Preparation of single cell suspensions from mouse samples

Spleens and TdLNs were mechanically disrupted by passing them through a 70 μ m cell strainer using the plunger of a 3 mL syringe and then resuspended in 1 mL of ACK red blood cell lysing buffer (Gibco NY, USA) for 3 min at room temperature (RT). The tumor was cut into pieces with scissors and then enzymatically digested with 1 mg per ml collagenase IV (Gibco, NY, USA) at 37 °C for 40 min. Following digestion, tissues were filtered through a 70 μ m cell strainer, and then resuspended in 40% Percoll (Cytiva, Cat. # 17-0891-01, MA, USA) for centrifugation at 1200 g for

20 min at RT, after which they were incubated with ACK red blood cell lysing buffer. All isolated cells were suspended in PBS supplemented with 2 mM EDTA and 1% FBS.

Flow cytometry

Surface markers were stained in PBS containing 2% BSA or FBS (w/v) at 4 °C for 30 min after Fc blocking (Invitrogen, Cat. # 14-0161-86, CA, USA) to characterize murine immune cell subsets. FVS700 (BD Biosciences, Cat. # 564,997, CA, USA) were used to discriminate the viable or non-viable cells according to the manufacturer's instructions. Intracellular cytokine staining (ICS) for IFN- γ and TNF- α were performed with the Cytofix/Cytoperm Fixation/Permeabilization Kit (BD Biosciences, Cat. #554,714, CA, USA). The following reagents were purchased from BD Biosciences (CA, USA): CD45-BV786 (Cat. # 564,225), CD3e-BUV737 (Cat. # 612,771), CD4-APC/Cy7 (Cat. # 552,051), CD8a-BV650 (Cat. # 563,234), CD44-BV510 (Cat. # 563,114), CD62L-PE/CF594 (Cat. # 562,404), CD80-BUV737 (Cat. # 612,773), CD86-BUV395 (Cat. # 564,199), Ly6G-PerCP/Cy5.5 (Cat. # 560,602), Foxp3-PE (Cat. # 566,881). The following reagents were purchased from Invitrogen (CA, USA): NK1.1-BUV395 (Cat. # 363-5941-82), KLRG1-PerCP/eF710 (Cat. # 46-5893-82), CD11c-PerCP/Cy5.5 (Cat. # 45-0114-82), B220-SB600 (Cat. # 63-0452-82), CD11b-APC/Cy7 (Cat. # A15390), Ly6C-eF450 (Cat. # 48-5932-82), H-2Kd/H-2Dd-FITC (Cat. # 11-5998-82). The following reagents were purchased from Biolegend (CA, USA): CD39-PE/Cy7 (Cat. # 143,806), IFN- γ -PE (Cat. # 505,808), IA/IE-BV510 (Cat. # 107,636), CD317-BV711 (Cat. # 127,039).

Immunohistochemical analysis

Immunohistochemistry was performed to detect CD8⁺ TILs of rechallenged tumor tissues. The tumor tissues were fixed in a 10% formalin solution, followed by embedding in paraffin, and then were cut into 4 μ m thick sections and mounted on poly-L-lysine coated slides. Subsequently, the slices were subjected to staining with Anti-mouse CD8 Abs (ABclonal, Wuhan, China).

Statistical analysis

SPSS version 22.0 (IBM Corporation, Armonk, NY, USA) and GraphPad Prism 9.0.0 software were used for the statistical analysis. Survival curves for PFS was estimated using the Kaplan–Meier method and the Chi-square or Fisher's exact test was employed to compare categorical variables via SPSS version 22.0. Statistical significance was determined using one-way analysis of variance (ANOVA) followed by Tukey's multiple comparisons test, and correlation analysis

was conducted using Pearson's test via GraphPad Prism 9.0.0 software (*, $p < 0.05$; **, $p < 0.01$; ***, $p < 0.001$).

Date availability

The data supporting the findings of this study are available from the corresponding author upon reasonable request.

Results

MWA combined ICI therapy yielded a favorable clinical outcome for patients with lung cancer

We have performed a retrospective analysis of two patient cohorts with lung cancer: one cohort received ICI monotherapy with Camrelizumab, while the other cohort underwent combined therapy with MWA and ICI. The baseline characteristics of the enrolled patients are presented in Table 1. No significant differences in basic characteristics, including, sex, age, smoking history, ECOG score, pathology, lymph nodes metastases, stage, PD-L1 expression or PD-L1 positive (TPS) were observed between the two groups. The median follow-up time is 9.07 months with no loss to follow-up. Our results revealed that patients receiving the combined therapy achieved a higher objective response rate (ORR) compared to those on ICI monotherapy [43.8% (14/32) vs. 16.7% (5/30), $p = 0.0208$] (Fig. 1A, B and S1). The PFS of the combined therapy group was markedly superior to that of the ICI monotherapy group (9.88 ± 6.95 [95% confidence interval, 8.92–13.7] vs. 5.32 ± 4.21 [95% confidence interval, 4.37–7.89] months, $p = 0.0012$) (Fig. 1C). Based on the above data, we have identified that patients with lung cancer underwent the combinational therapy represented a highly promising treatment regimen than those underwent the monotherapy.

MWA monotherapy was insufficient to inhibit rechallenged tumor growth but upregulated PD-L1 expression on rechallenge tumor

To investigate the impact of MWA on immune activation and memory, we utilized a post-MWA tumor rechallenged model [24, 25]. In this experimental setup, murine Lewis lung carcinoma (LLC) cells were initially inoculated into the left flank of the mice to establish the primary tumor, designated as Day -9. Subsequently, after MWA therapy was administered to this primary tumor, denoted as Day 0, LLC cells were inoculated into the right flank on the same Day 0 to form a rechallenged tumor. This experimental paradigm was strategically designed to evaluate the immune response and memory (Fig. 2A). Our findings revealed that following treatment with MWA alone, although the primary tumor

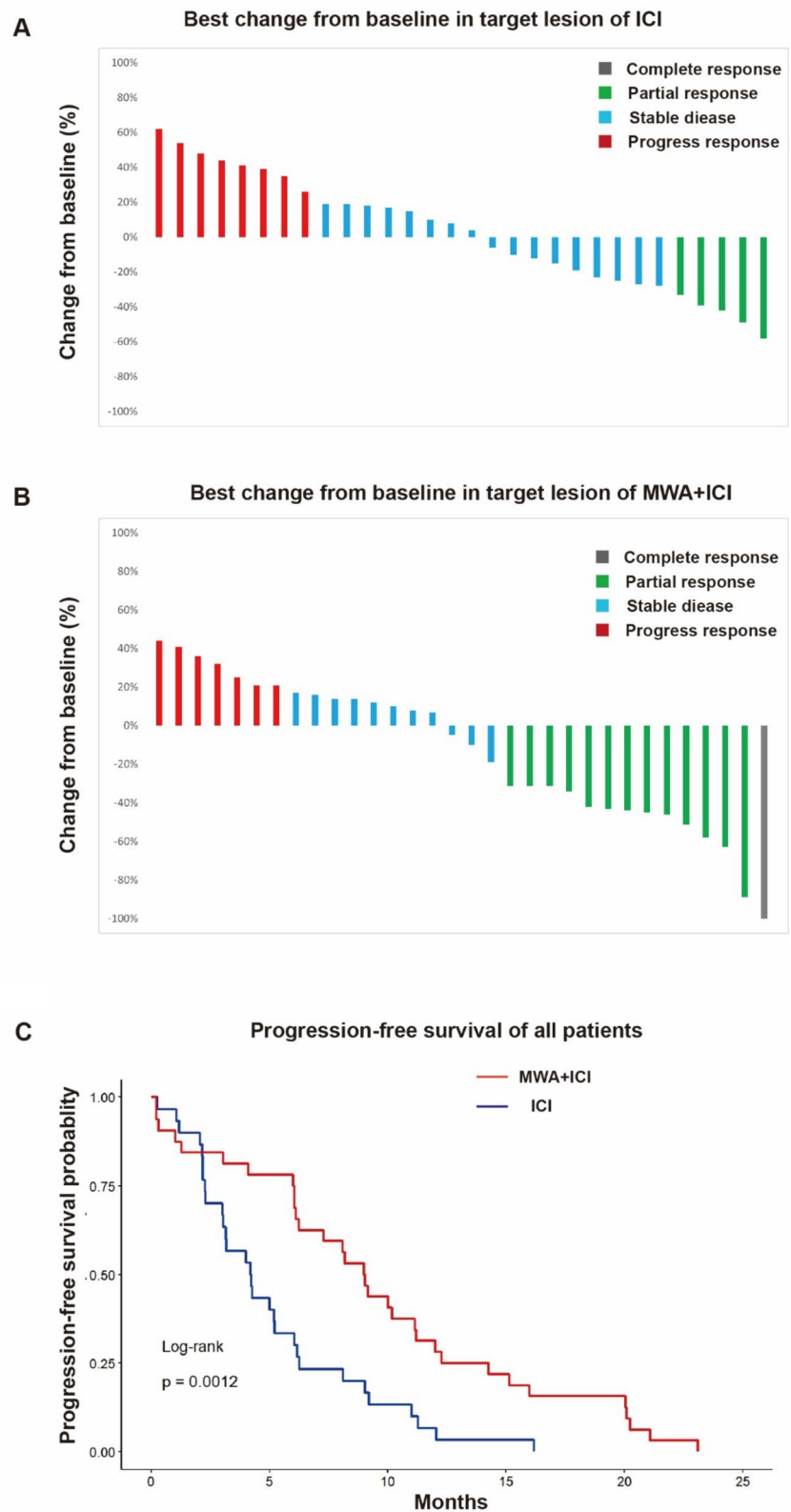
was effectively locally ablated, MWA did not prevent the growth of the rechallenged tumor when compared to Un group (Fig. 2B–D), implying that MWA does not elicit a long-lasting anti-tumor immune memory in our study. Certainly, although there was no inhibition of the rechallenged tumor growth, MWA destroyed the primary tumor. This resulted in the tumors in the Un group reaching the laboratory animal ethics standards earlier. Ultimately, the survival rate of the mice in the MWA group was higher than that of the Un group, which highlights the advantage of MWA as a local treatment modality (Fig. 2E). One of the main mechanisms by which tumor cells evade immune detection involves the upregulation of immunosuppressive checkpoints on tumor surface, such as PD-L1 [26]. Therefore, we examined the expression of PD-L1 on the rechallenged tumors. For the first time, we observed that PD-L1 expression on the rechallenge tumors was upregulated following MWA treatment (Fig. 2F, G). In conclusion, our results indicated that although MWA is effective in removing local tumors, it fails to guard against tumor rechallenge and could potentially worsen the immune evasion of the rechallenge tumor with upregulated PD-L1 expression.

The combination of MWA with α PD-L1 therapy demonstrated a synergistic increase in antitumor efficacy within rechallenged tumor mouse model

Given the increase of PD-L1 expression on the rechallenged tumors after the primary tumor had undergone MWA, we employed a combination of MWA and anti-PD-L1 antibody (α PD-L1) to bolster resistance against tumor rechallenge. In our established rechallenge model, α PD-L1 treatment was initiated after the day of tumor rechallenge, designated as Day 1 (Fig. 3A). Mice was treated with MWA, α PD-L1 or MWA + α PD-L1 (M + α P). Our results revealed that the combinational therapy significantly suppressed the growth of the rechallenged tumor, and also resulted in a reduction in tumor recurrence after concurrent treatment (Fig. 3B, C, E). Furthermore, in terms of survival, MWA effectively eradicated the primary tumor and extended the survival of mice beyond that of the α PD-L1 group. Additionally, the combinational therapy exhibited a longer survival compared to either monotherapy alone (Fig. 3D).

CD8⁺T cells are the primary executors of antitumor immune responses [27]; Immunohistochemical analysis of the rechallenged tumors revealed a marked increase in the infiltration of CD8⁺ TILs within the combination group (Fig. 3F and S2E). To further characterize the tumor immune microenvironment, we performed multiparametric flow cytometry analysis to quantify CD8⁺ T cell populations in tumor tissues. Notably, the combination therapy elicited a significant increase in the frequency of CD8⁺ TILs (Figure S2A–B). Furthermore, this therapeutic strategy

Fig. 1 Clinical response to ICI monotherapy and MWA combined with ICI. **A, B** Waterfall plot of best response change in tumor burden from baseline patients. **C** Kaplan–Meier curves of the progression-free survival in both groups of patients. *Note:* Quantitative variables are expressed as means and range



substantially augmented their functional capacity, as evidenced by enhanced IFN- γ secretion (Figure S2C-D). These data collectively indicate that the combined regimen not only

promotes CD8⁺ T cell infiltrating into the tumor but also potentiates their effector functions. In addition, to confirm whether the antitumor efficacy of the combinational therapy

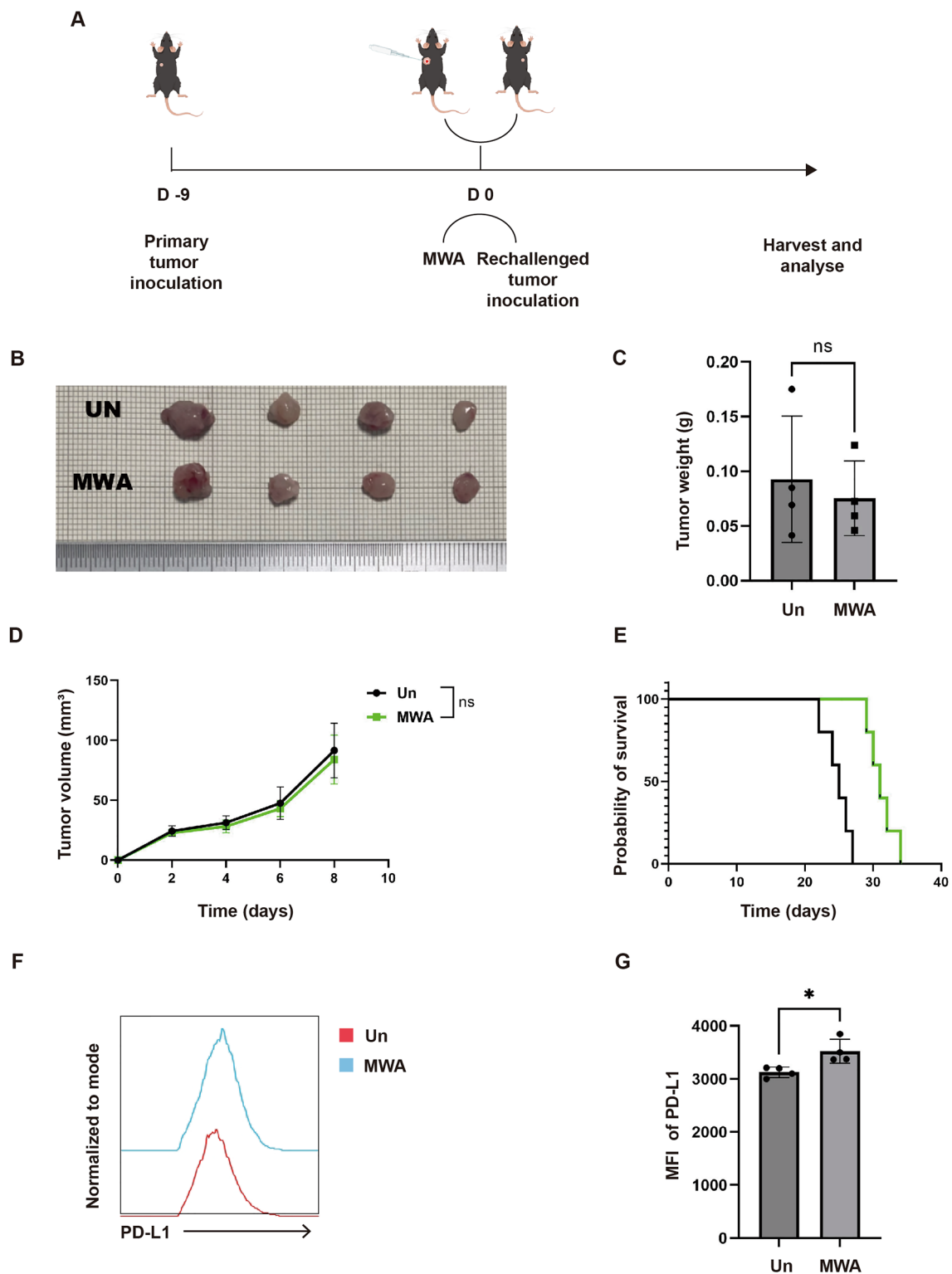


Fig. 2 Microwave ablation monotherapy fails to suppress the growth of rechallenged tumor but upregulates PD-L1 expression on tumor cells. **A** Graphical depiction of the experimental setup and procedural outline for the B-F experimental series. **B** Photographic visualization of the rechallenged tumor across various experimental groups. **C**, **D**

Daily tumor volume measurements and tumor weight assessments following tumor rechallenge. **E** The survival of mice within a tumor rechallenged experimental model. **F** Flow cytometric analysis of the level of PD-L1 expression on rechallenged tumor cells after MWA. **G** Statistical results for F. (*, $p < 0.05$)

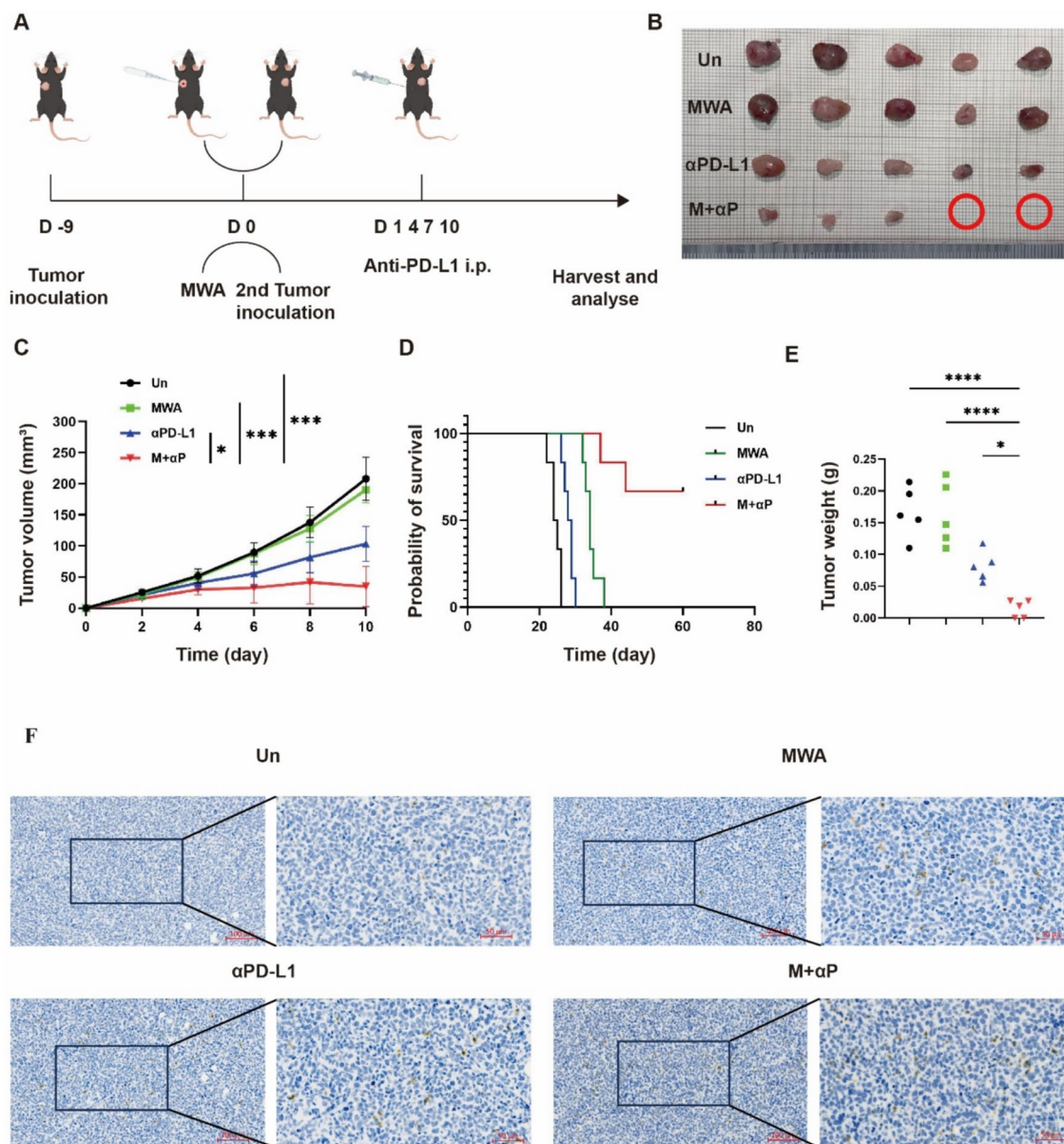


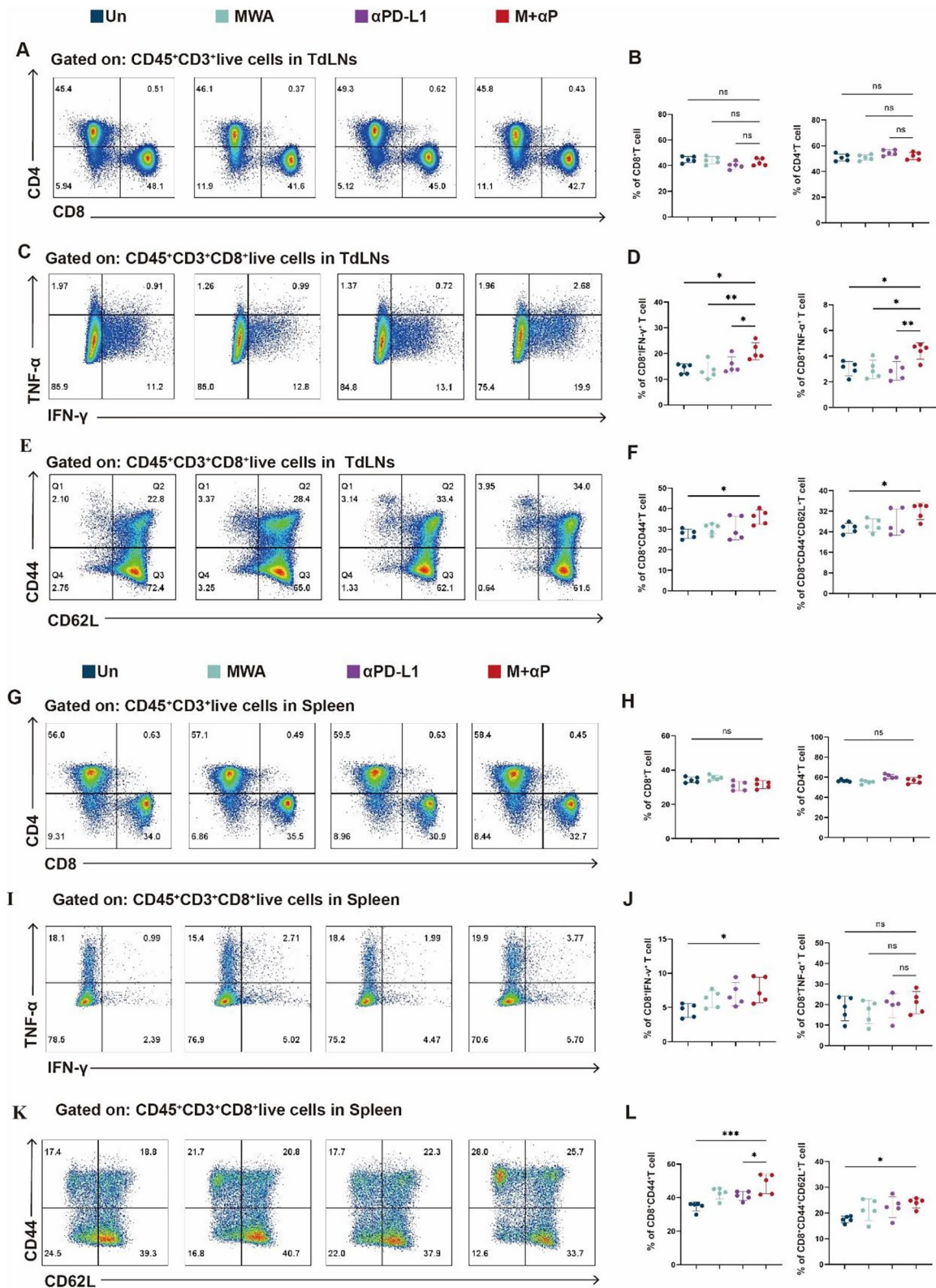
Fig. 3 The combination of MWA with α PD-L1 therapy elicits a robust resistance against rechallenged tumor, yielding favorable therapeutic outcomes. **A** Graphical depiction of the experimental setup and procedural outline for the B-D experimental series. **B** Photographic visualization of the rechallenged tumor across various experimental groups. **C** Daily tumor volume measurements following tumor rechall-

enge. **D** The survival of mice within a tumor rechallenged experimental model. **E** The statistical analysis delineating the quantification of rechallenged tumor weights. **F** Immunohistochemical staining of CD8⁺ T cells within rechallenged tumor in all treatment groups (*, $p < 0.05$; ***, $p < 0.001$; ****, $p < 0.0001$).

was dependent on CD8⁺ T cells, we further employed a CD8⁺ T cell depletion antibody and found that the combination therapy were unable to control rechallenged tumor after CD8⁺ T cell depletion (Figure S2F-I). In summary, the combination therapy enhances the antitumor effect by increasing the infiltration of CD8⁺ T cells into the tumor, augmenting the anti-tumor function of CD8⁺ T cells, and exerting a synergistic antitumor effect. Moreover, this synergistic effect is dependent on CD8⁺ T cells.

The combination of MWA with α PD-L1 therapy augmented the function of CD8⁺ T cells within TdLNs

TdLNs represent the initiatory and sustaining site of the body's antitumor immune response and are crucial for the induction of tolerance to tumors by the immune system [28, 29]. To further investigate the antitumor immunity elicited by combination therapy, we examined the immunological microenvironment within TdLNs. CD8⁺ T cells are one



of the effector target populations for PD-L1 [30]. Our initial assessment of TdLNs revealed that the percentage of CD8⁺ T cells or CD4⁺ T cells did not change significantly

(Fig. 4A, B). TdLNs consistently serve as a reservoir for T cells, maintaining both the abundance and heterogeneity of the cellular population [31]. Cytotoxicity is critical for the

Fig. 4 The MWA combined with α PD-L1 therapy enhanced the antitumor function of CD8⁺ T cells. **A** The proportion of CD4⁺ T cells or CD8⁺ T cells within TdLNs, as shown in flow cytometry plot. **B** Statistical results for A. **C** The proportion of IFN- γ ⁺CD8⁺ T cells or TNF- α ⁺CD8⁺ T cells within TdLNs, as shown in flow cytometry plots. **D** Statistical results for C. **E** The proportion of CD44⁺CD62L⁺CD8⁺ T cells (CD8⁺ T central memory, TCM) or CD44⁺CD62L⁻CD8⁺ T cells (CD8⁺ T effector memory, TEM) within TdLNs, as shown in flow cytometry plots. **F** Statistical results for E. **G** The proportion of CD4⁺ T cells or CD8⁺ T cells within spleen, as shown in flow cytometry plot. **H** Statistical results for G. **I** The proportion of IFN- γ ⁺CD8⁺ T cells or TNF- α ⁺CD8⁺ T cells within spleen, as shown in flow cytometry plots. **J** Statistical results for I. **K** The proportion of CD44⁺CD62L⁺CD8⁺ T cells (TCM) and CD44⁺CD62L⁻CD8⁺ T cells (TEM) within spleen, as shown in flow cytometry plots. **L** Statistical results for K (*, $p < 0.05$; **, $p < 0.01$; ***, $p < 0.001$)

antitumor function of CD8⁺ T cells. We found that the cytotoxic capabilities of CD8⁺ T cells were notably enhanced following combinational therapy, with a significant increase in the secretion of IFN- γ and TNF- α compared to monotherapy (Fig. 4C, D). Moreover, combinational therapy significantly increased the proportion of T memory cells, particularly CD8⁺ T central memory (CD8⁺ CD44⁺ CD62L⁺, Tcm) (Fig. 4E, F). Concurrently, we observed changes in the peripheral spleen, where the percentage of CD8⁺ T cells or CD4⁺ T cells did not change significantly (Fig. 4G, H). Functionally, there was a marked increase in the proportion of IFN- γ ⁺CD8⁺ T cells in combinational therapy, and the proportion of TNF- α ⁺CD8⁺ T cells an increasing trend, although it did not reach statistical significance (Fig. 4I, J). The proportions of memory T cells, Tcm, were also elevated within the spleen (Fig. 4K, L). Additionally, we examined the population of regulatory T cells (Tregs) with immunosuppressive function within TdLNs and the spleen. The results indicated that there was no significant difference in the Treg population, either within TdLNs or the spleen (Figure S4A–D), suggesting that the combination therapy did not have a discernible effect on the Treg population. In summary, combination therapy enhanced the function of CD8⁺ T cells within both TdLNs and the peripheral (spleen), elevated the ratios of Tcm cells, and effectively bolstered the resistance to tumor rechallenge.

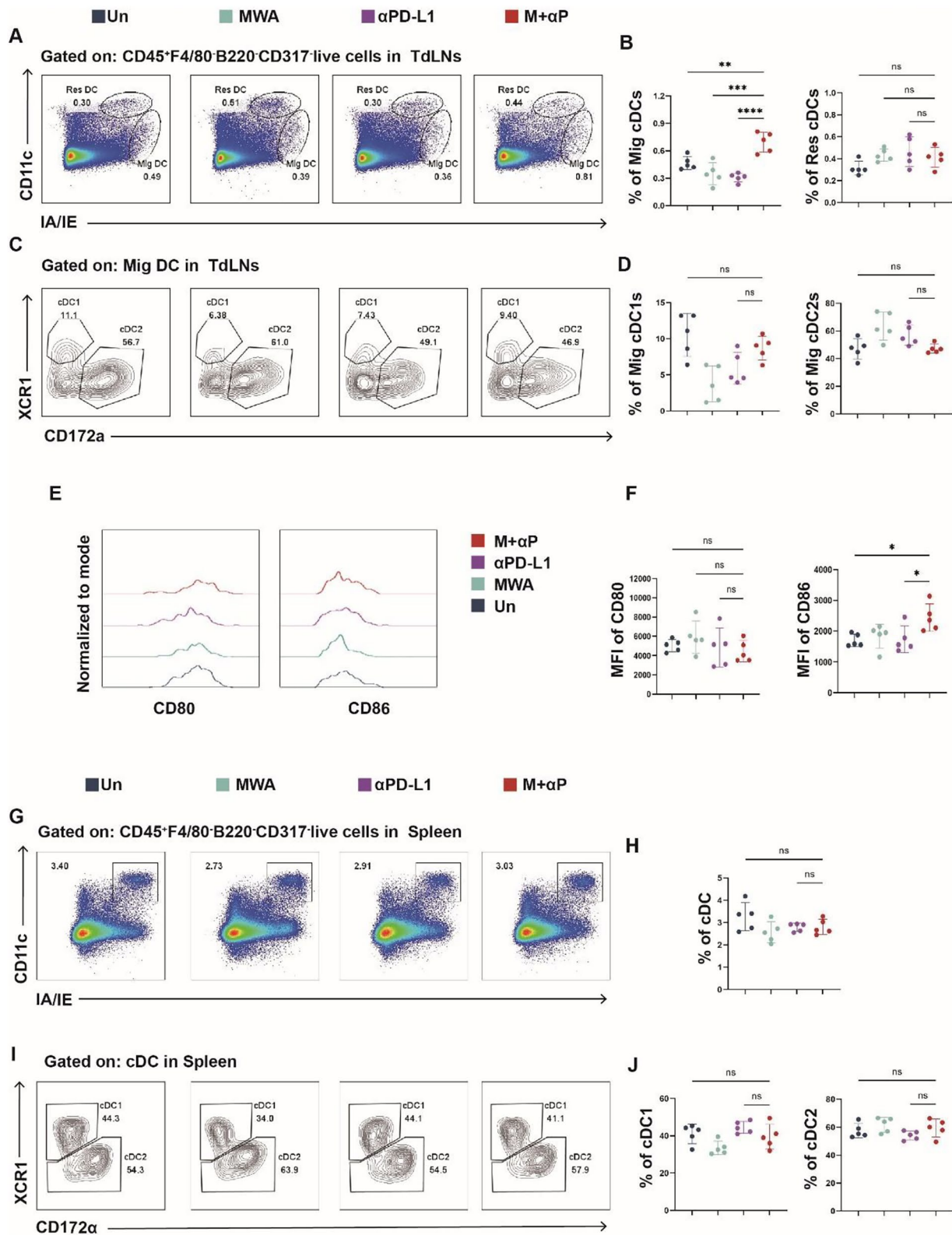
Combining MWA with α PD-L1 increased the proportion of migratory DCs in TdLNs and promoted DC1 activation.

Conventional Dendritic Cell Type (cDCs) are a specialized subset of antigen-presenting cells within the immune system, capable of capturing antigens in the body's peripheral tissues and presenting them to T cells. This function allows cDCs to act as a critical bridge between the innate and adaptive immune responses [32]. MWA ablates tumors and induces antigens release, where cDCs phagocytosed these antigens.

Subsequently cDCs migrated to TdLNs for antigen presentation. Within these TdLNs, cDCs are generally categorized into two types: resident DCs (CD11c^{hi}MHC-II^{int}, Res DC), which are in an immature state, and migratory DCs (CD11c^{int}MHC-II^{hi}, Mig DC), which are mature and primarily responsible for antigen presentation [33]. We therefore conducted a detection and analysis of DC subsets within TdLNs and found that neither monotherapy nor combined therapy significantly affected the proportion of resident DCs in TdLNs. However, combined therapy markedly increased the proportion of Mig DCs compared to monotherapy (Fig. 5A, B). Furthermore, we observed that monotherapy reduced the proportion of cDC1 (XCR1⁺) within Mig DCs and increased the proportion of cDC2 (Fig. 5D), whereas combined therapy restored the proportion of cDC1 and also increased the CD86 expression on cDC1 within migratory DCs (Fig. 5C–F). In contrast, such results were not observed in the spleen, where no significant changes were observed in the overall cDC population, nor in cDC1 or cDC2 subsets (Fig. 5G–J). Concurrently, we examined TdLNs on the side of MWA, referred to as MWA-TdLNs, and the results were essentially consistent with the previous findings (Figure S3). In summary, our findings indicated that combined therapy increased the proportion of Mig DCs in TdLNs, restored the proportion of cDC1, and promoted their activation.

Enhanced efficacy of combined therapy was dependent on the migration of lymphocytes from TdLNs to tumor

TdLNs serve as a critical reservoir for initiating anti-tumor immunity, where a significant population of T cells is stimulated by tumor antigens. These T cells then migrate to the tumor site, where they evolve into effector T cells capable of exerting cytotoxic effects against tumor cells [31]. During this process, the migration of immune cells from TdLNs to tumor site plays a pivotal role. FTY720 (fingolimod), a novel immunosuppressive agent, primarily functions by binding to the sphingosine-1-phosphate receptor (S1P receptor), thereby inhibiting the migration of lymphocytes, particularly T cells, into the tumor [34, 35]. To investigate whether the migration of immune cells from TdLNs is essential for the augmented efficacy of MWA combined with α PD-L1 therapy, we designed experiments with untreated, MWA + α PD-L1, and MWA + α PD-L1 + FTY720 treatment groups (Fig. 6A). Monitoring tumor growth revealed that the addition of FTY720 abrogated the therapeutic effects of the combined treatment, resulting in uncontrolled tumor growth (Fig. 6B–D). Flow cytometric analysis of the tumor and TdLNs demonstrated that the combined treatment significantly increased the infiltration of CD3⁺ T cells within the tumor, whereas FTY720 treatment markedly reduced this infiltration (Fig. 6E–G). Furthermore, following



MWA + α PD-L1 treatment, we observed an elevated proportion of CD8⁺ T cells and a decreased proportion of CD4⁺ T cells within the tumor (Fig. 6E–G). In summary, our findings

demonstrate that the therapeutic efficacy of MWA in combination with α PD-L1 therapy is dependent on the migration of lymphocytes from TdLNs to tumor.

Fig. 5 MWA in conjunction with α PD-L1 therapy increased the proportion of migratory dendritic cells (Mig DCs) within the TdLNs and facilitated their activation. **A** Graphical representations of the proportional distribution of DC subsets within TdLNs at post-curative treatment intervention. **B** Statistical results for A. **C** Graphical representations of the proportional distribution of DC subsets within Mig DC. **D** Statistical results for C. **E** The median fluorescence intensity (MFI) of CD80 and CD86 expression on Mig cDC1s in TdLNs following the combination of MWA with α PD-L1 therapy. **F** Statistical results for E. **G** Graphical representations of the proportional distribution of DCs within spleen. **H** Statistical results for G. **I** Graphical representations of the proportional distribution of DC subsets within cDC in spleen. **J** Statistical results for I (*, $p < 0.05$; **, $p < 0.01$; ***, $p < 0.001$; ****, $p < 0.0001$)

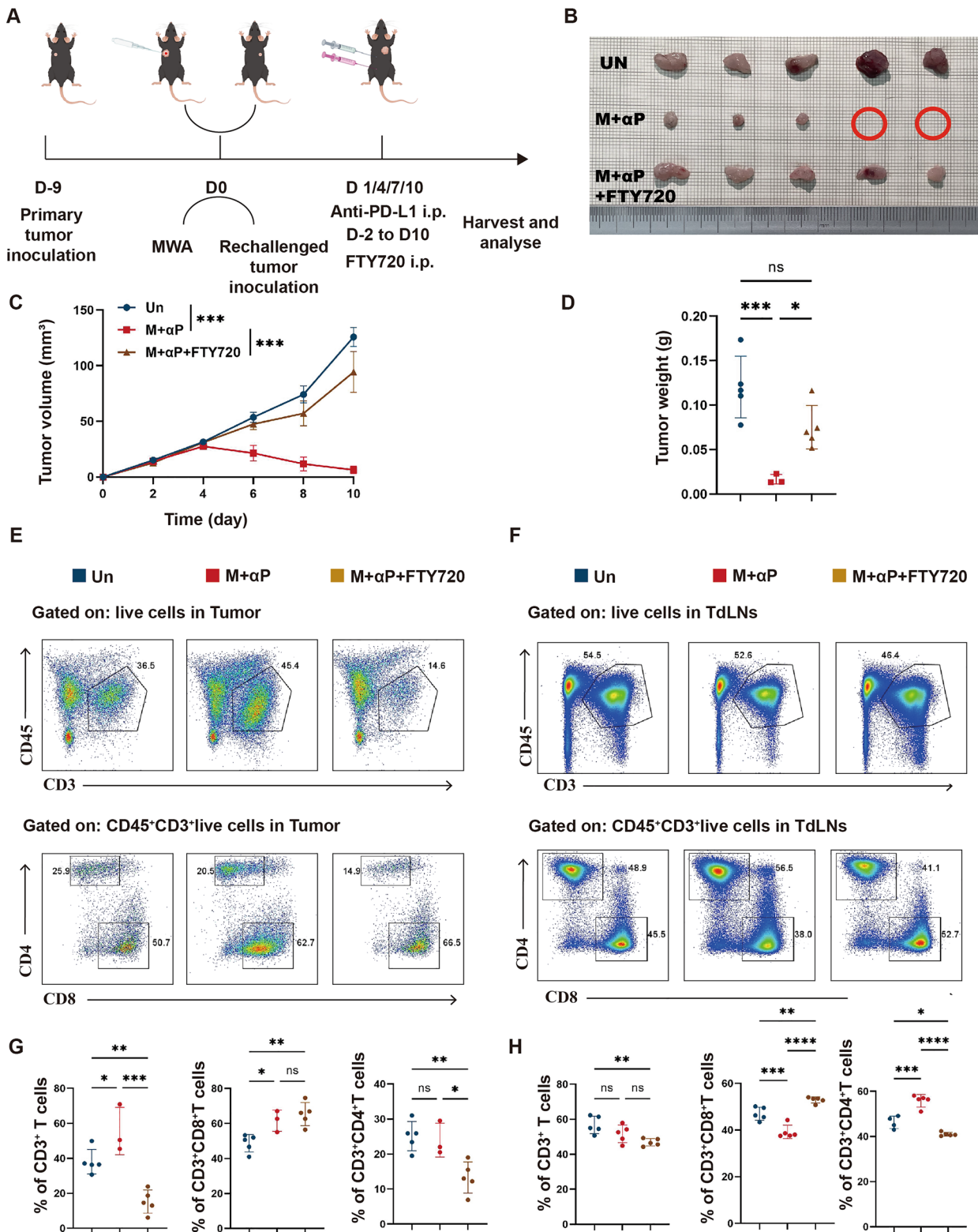
Discussion

In recent years, MWA has increasingly demonstrated its therapeutic advantages in the treatment of pulmonary tumors, owing to its unique treatment benefits [4, 36]. Our team conducted a retrospective analysis of patients with oligometastatic NSCLC who underwent MWA following complete surgical resection. The median PFS and overall survival (OS) for these patients were 15.1 months and 40.6 months, respectively. These results indicated that MWA is a safe and effective option for selected patients with pulmonary oligorecurrence after radical surgical resection of NSCLC [21]. In this study, we performed a retrospective analysis of two advanced NSCLC patients cohorts: one receiving ICI monotherapy and MWA combined with ICI. The results demonstrated that the combination therapy yielded a higher ORR and superior PFS, suggesting that the combined treatment regimen holds significant therapeutic potential to improve clinical efficacy for advanced NSCLC patients. Furthermore, the results suggested that MWA induces alterations in the tumor microenvironment, which contain positive, proactive elements that can enhance the efficacy of monotherapy with ICI.

To further investigate the mechanisms of combination therapy, we established a tumor rechallenged model. In this model, tumor cells were reimplanted in the contralateral side of the mouse after MWA treatment. This model not only simulated the condition of advanced stage patients to explore the synergistic effects of combined therapy but also replicated post-MWA tumor recurrence, allowing us to assess whether the combination treatment can resist tumor relapse. In this study, we observed that while MWA monotherapy effectively eliminated the primary tumor, it concurrently upregulated PD-L1 expression in rechallenged tumors. A similar upregulation of PD-L1 was also noted following RFA [20]. This phenomenon may contribute to the recurrence of tumors post-ablation. Therefore, it is necessary to combine MWA with PD-1/PD-L1 antibody therapy for those patients who exhibit higher PD-L1 expression in their tumors. CD8⁺TILs served as a critical biomarker for

assessing immune therapeutic efficacy. And our findings indicate combinatorial regimen exerted antitumor effects by enhancing CD8⁺TIL infiltration and augmenting effector functionality. Furthermore, the therapeutic efficacy was abrogated when CD8⁺ T cells were depleted, highlighting the reliance of the combined treatment on the presence of CD8⁺ T cells. Previous research has shown that the antitumor effects of MWA in combination with α PD-L1 are mediated by the IFN- γ -CXCL9-CD8⁺ T cell axis [37]. In addition, there has been a growing interest in combining MWA with various immunotherapies, such as ICIs, Chimeric Antigen Receptor T-cell (CAR-T) therapy, and immunoadjuvants, to explore the synergistic effects of these combined treatments [7]. MWA, when combined with plus adoptive Th9 cell transfer therapy, has effectively inhibited the recurrence of NSCLC tumors [25]. The integration of MWA with ICIs has been demonstrated to effectively prolong survival and enhance the presence of CD8⁺ TILs [38]. Furthermore, the combination of MWA with CAR-T therapy has been shown to remodel the tumor microenvironment, augment the mitochondrial oxidative metabolism of CD8⁺ TILs, and thereby potentiate the therapeutic efficacy in NSCLC [39]. The therapeutic synergy of MWA and Flt3L markedly curbs tumor recurrence by harnessing a CD8⁺ central memory T (Tcm)-like cell-mediated antitumor immune response within TdLNs [40]. The pairing of MWA with IL-21 demonstrated a potent abscopal anti-tumor effect, significantly augmenting the effector function of CD8⁺ T cells [34]. These results collectively elucidated the partial mechanisms of synergistic efficacy from various perspectives and concurrently addressed the issue of post-ablation recurrence.

Extensive evidence substantiated the concept that TdLNs function as essential peripheral immune organs. Within the TdLNs, antigen-presenting cells (APCs), mainly DCs, facilitated the presentation of antigens to T cells, a process that is critical for the survival, activation, and functional differentiation of T cells. In early-stage NSCLC, MWA effectively destroyed the tumor while preserving the integrity of the lymph nodes. This allowed for the antigens released post-ablation, such as tumor-associated antigens, heat shock proteins, and high mobility group protein 1, to be efficiently processed by APCs within the TdLNs. Notably, the activation of CD8⁺ T cells within the TdLNs was crucial for maintaining robust anti-tumor immune responses [41]. To this end, we have focused on assessing the immune microenvironment within the TdLNs. Our findings revealed that the proportion of CD8⁺ and CD4⁺ T cells within the TdLNs remained relatively stable following combined therapy; however, there was a significant increase in the secretion capacity of IFN- γ and TNF- α . Additionally, we observed a marked increase in the proportion of CD44⁺CD8⁺ T cells or CD44⁺CD62L⁺CD8⁺ Tcm cells post-combination treatment. Our results further demonstrated that the antitumor



efficacy was dependent on the presence of TdLNs, underscoring the role of TdLNs as a reservoir that continuously supplies effector and memory-related T cells, thereby

facilitating rapid and effective anti-tumor responses. Tcm as a distinct subset of memory T cells that play a crucial role in the adaptive immune response [42, 43]. Recent studies have

Fig. 6 FTY720 abrogates the therapeutic efficacy of combined MWA and α PD-L1 therapy on rechallenged tumor. **A** Graphical depiction of the experimental setup and procedural outline for the B-D experimental series. **B** Photographic visualization of the rechallenged tumor across various experimental groups. **C, D** Daily tumor volume measurements and tumor weight assessments following tumor rechallenge. **E** The proportion of CD3⁺, CD4⁺ or CD8⁺ T cells within the rechallenged tumor, as shown in flow cytometry plot. **F** The proportion of CD3⁺, CD4⁺ or CD8⁺ T cells within TdLNs, as shown in flow cytometry plot. **G** Statistical results for E. **H** Statistical results for F (*, $p < 0.05$; **, $p < 0.01$; ***, $p < 0.001$; ****, $p < 0.0001$)

emphasized the critical role of Tcm cells in responding to PD-1/PD-L1 antibody therapy. These Tcm cells can rapidly react to antigenic challenges, providing long-lasting protective functions and enhancing the response to tumor re-challenge [44]. Concomitantly, we observed similar phenomena within the spleen. Previous research has demonstrated that the combination of 2-deoxy-D-glucose (2DG) with MWA exerted anti-tumor effects within LNs by activating STAT-1 and thereby promoting the differentiation of Tcm [45]. Additionally, it has been found that inhibiting glycolysis after MWA can promote the differentiation of peripheral Tcm in breast cancer patients [45].

Conventional Dendritic Cell Type 1 (cDC1) plays a crucial role in modulating anti-tumor T cell responses during the activation phase within TdLNs [46]. We examined the DC subsets within the TdLNs and found that combined therapy significantly enhanced the recruitment of Mig DCs, while exerting a minimal effect on Res DCs. Notably, monotherapy appeared to constrain Mig cDC1 populations, which were restored to normal levels following combined treatment. Additionally, we observed that combined therapy promoted the activation of Mig cDC1 cells. However, in the spleen, no significant differences were observed in the overall cDC populations or in specific subpopulations. Previous studies have reported that under naive and tumor-bearing conditions, the expression of PD-L1 on cDC1 within the spleen remains unchanged and is maintained at a relatively low level [47]. This may account for the minimal changes observed in the spleen after treatment.

Based on the changes in the tumor immune microenvironment and TdLNs, we employed FTY720 to block the migration of T cells from TdLNs to the tumor [48]. The results confirmed that the loss of T cells within TdLNs negates the efficacy of the combined therapy. After MWA, the release of antigens is observed, which are then taken up by Mig DC1 and subsequently transported to TdLNs. Within the TdLN microenvironment, Mig DC1 presents these antigens to naive T cells, which further differentiate into Tcm cells. Under the combined therapy regimen, Tcm cells are primed to respond more rapidly to tumor rechallenge, differentiating into effector T cells and migrating to the tumor site to exert antitumor effects. Consequently, the preservation of TdLNs

may emerge as a new trend in the future, given their crucial role in the generation of systemic anti-tumor immunity.

Despite the progress made, several significant limitations remain. First, although the efficacy of combined therapy has been identified through clinical retrospective studies, validation has thus far been limited to animal models. Future investigations should incorporate clinical patient samples to provide confirmation. Second, while we have observed that combined therapy increases the infiltration of CD8⁺ T cells within tumors, a detailed description of the exhaustion state of these CD8⁺ T cells in response to combined therapy is lacking. Moreover, this represented merely one of the multiple mechanisms contributing to the efficacy of the combined therapeutic regimen. The specific differentiation of Tcm within TdLNs, as well as the interactions between DCs and T cells, remain unclear and warrant further exploration.

In conclusion, our study has demonstrated that the combination of MWA with ICIs showed a promising therapeutic efficacy. In preclinical models, we have identified one of the causes of post-ablation recurrence and successfully addressed this issue with the combination of MWA and α PD-L1 blockade. Furthermore, we have explored the potential mechanisms underlying the enhanced efficacy of this combination for treating advanced-stage patients. Importantly, the efficacy of the combined treatment was contingent upon the presence of TdLNs. Future research was warranted to further explore and amplify this promising combinational regime.

Supplementary Information The online version contains supplementary material available at <https://doi.org/10.1007/s00262-025-04003-5>.

Acknowledgements None

Author contribution Fengkuo Xu, Jing Sang and Nan Wang contributed equally to this work and should be considered co-first authors. Fengkuo Xu, Jing Sang, Meixiang Wang, Ji Ma and Huanan Chen performed the animal experiments. Nan Wang and Yahan Huang collected clinical data. Fengkuo Xu, Jing Sang and Nan Wang analyzed the data and prepared a table and all figures. Fengkuo Xu and Jing Sang wrote this manuscript. Qi Xie, Zhigang Wei, and Xin Ye conceived, designed, and supervised the project and contributed equally to this work.

Funding National Natural Science Foundation of China, 82072028

Data availability No datasets were generated or analysed during the current study.

Declarations

Conflict of interest The authors declare no competing interests.

Open Access This article is licensed under a Creative Commons Attribution-NonCommercial-NoDerivatives 4.0 International License, which permits any non-commercial use, sharing, distribution and reproduction in any medium or format, as long as you give appropriate credit to the original author(s) and the source, provide a link to the Creative Commons licence, and indicate if you modified the licensed material. You do not have permission under this licence to share adapted material

derived from this article or parts of it. The images or other third party material in this article are included in the article's Creative Commons licence, unless indicated otherwise in a credit line to the material. If material is not included in the article's Creative Commons licence and your intended use is not permitted by statutory regulation or exceeds the permitted use, you will need to obtain permission directly from the copyright holder. To view a copy of this licence, visit <http://creativecommons.org/licenses/by-nc-nd/4.0/>.


References

- Bray F, Laversanne M, Sung H, Ferlay J, Siegel RL, Soerjomataram I, Jemal A (2024) Global cancer statistics 2022: GLOBOCAN estimates of incidence and mortality worldwide for 36 cancers in 185 countries. *CA Cancer J Clin* 74:229–263. <https://doi.org/10.3322/caac.21834>
- Riely GJ, Wood DE, Ettinger DS et al (2024) Non-small cell lung cancer, version 4.2024, NCCN clinical practice guidelines in oncology. *J Natl Compr Canc Netw* 22:249–274. <https://doi.org/10.6004/jnccn.2204.0023>
- Elsayed M, Solomon SB (2023) Interventional oncology: 2043 and beyond. *Radiology* 308:e230139. <https://doi.org/10.1148/radiol.230139>
- Ye X, Fan W, Wang Z et al (2022) Clinical practice guidelines on image-guided thermal ablation of primary and metastatic lung tumors (2022 edition). *J Cancer Res Ther* 18:1213–30. https://doi.org/10.4103/jcrt.jcrt_880_22
- Xu F, Wei Z, Ye X (2024) Immunomodulatory effects of microwave ablation on malignant tumors. *Am J Cancer Res* 14:2714–2730. <https://doi.org/10.62347/QJID8425>
- Rangamwa K, Leong T, Weeden C et al (2021) Thermal ablation in non-small cell lung cancer: a review of treatment modalities and the evidence for combination with immune checkpoint inhibitors. *Transl Lung Cancer Res* 10:2842–2857. <https://doi.org/10.21037/tlcr-20-1075>
- Xie L, Meng Z (2023) Immunomodulatory effect of locoregional therapy in the tumor microenvironment. *Mol Ther* 31:951–969. <https://doi.org/10.1016/j.ymthe.2023.01.017>
- Xu H, Sun W, Kong Y, Huang Y, Wei Z, Zhang L, Liang J, Ye X (2020) Immune abscopal effect of microwave ablation for lung metastases of endometrial carcinoma. *J Cancer Res Ther* 16:1718–1721. https://doi.org/10.4103/jcrt.JCRT_1399_20
- Abdalla EK, Vauthey JN, Ellis LM, Ellis V, Pollock R, Broglio KR, Hess K, Curley SA (2004) Recurrence and outcomes following hepatic resection, radiofrequency ablation, and combined resection/ablation for colorectal liver metastases. *Ann Surg* 239:818–25. <https://doi.org/10.1097/01.sla.0000128305.90650.71>
- Ribas A, Wolchok JD (2018) Cancer immunotherapy using checkpoint blockade. *Science* 359:1350–1355. <https://doi.org/10.1126/science.aar4060>
- Wang K, Coutifaris P, Brocks D et al (2024) Combination anti-PD-1 and anti-CTLA-4 therapy generates waves of clonal responses that include progenitor-exhausted CD8(+) T cells. *Cancer Cell* 42(1582–97):e10. <https://doi.org/10.1016/j.ccell.2024.08.007>
- Meyer ML, Fitzgerald BG, Paz-Ares L, Cappuzzo F, Janne PA, Peters S, Hirsch FR (2024) New promises and challenges in the treatment of advanced non-small-cell lung cancer. *Lancet* 404:803–822. [https://doi.org/10.1016/S0140-6736\(24\)01029-8](https://doi.org/10.1016/S0140-6736(24)01029-8)
- Gao J, Zhang C, Wei Z, Ye X (2023) Immunotherapy for early-stage non-small cell lung cancer: a system review. *J Cancer Res Ther* 19:849–865. https://doi.org/10.4103/jcrt.jcrt_723_23
- Li Y, Liang X, Li H, Chen X (2023) Efficacy and safety of immune checkpoint inhibitors for advanced non-small cell lung cancer with or without PD-L1 selection: a systematic review and network meta-analysis. *Chin Med J (Engl)* 136:2156–2165. <https://doi.org/10.1097/CM9.0000000000002750>
- Wei Z, Yang X, Ye X et al (2020) Microwave ablation plus chemotherapy versus chemotherapy in advanced non-small cell lung cancer: a multicenter, randomized, controlled, phase III clinical trial. *Eur Radiol* 30:2692–2702. <https://doi.org/10.1007/s00330-019-06613-x>
- Shi Q, Zhou X, Zhang Z et al (2022) Microwave ablation and synchronous transarterial chemoembolization combined with PD-1 inhibitor in patients with hepatocellular carcinoma following tyrosine kinase inhibitor intolerance. *Front Immunol* 13:1097625. <https://doi.org/10.3389/fimmu.2022.1097625>
- Huang ZM, Han X, Wang J et al (2024) A prospective, single-arm, phase 2 study of modified transarterial chemoembolization using low-dose chemotherapy with blank microspheres plus low-dose lenvatinib and microwave ablation in patients with large (>=7 cm) unresectable hepatocellular carcinoma: The TALEM Trial. *Liver Cancer* 13:438–450. <https://doi.org/10.1159/000536518>
- Laeseke P, Ng C, Ferko N et al (2023) Stereotactic body radiation therapy and thermal ablation for treatment of NSCLC: a systematic literature review and meta-analysis. *Lung Cancer* 182:107259. <https://doi.org/10.1016/j.lungcan.2023.107259>
- Shao D, Chen Y, Huang H, Liu Y, Chen J, Zhu D, Zheng X, Chen L, Jiang J (2022) LAG3 blockade coordinates with microwave ablation to promote CD8(+) T cell-mediated anti-tumor immunity. *J Transl Med* 20:433. <https://doi.org/10.1186/s12967-022-03646-7>
- Shi L, Chen L, Wu C et al (2016) PD-1 blockade boosts radiofrequency ablation-elicited adaptive immune responses against tumor. *Clin Cancer Res* 22:1173–1184. <https://doi.org/10.1158/1078-0432.CCR-15-1352>
- Ni Y, Peng J, Yang X, Wei Z, Zhai B, Chi J, Li X, Ye X (2021) Multicentre study of microwave ablation for pulmonary oligorecurrence after radical resection of non-small-cell lung cancer. *Br J Cancer* 125:672–678. <https://doi.org/10.1038/s41416-021-01404-y>
- Wei Z, Chi J, Cao P, Jin Y, Li X, Ye X (2023) Microwave ablation with a blunt-tip antenna for pulmonary ground-glass nodules: a retrospective, multicenter, case-control study. *Radiol Med* 128:1061–1069. <https://doi.org/10.1007/s11547-023-01672-z>
- Sang J, Liu P, Wang M, Xu F, Ma J, Wei Z, Ye X (2024) Dynamic changes in the immune microenvironment in tumor-draining lymph nodes of a Lewis lung cancer mouse model after microwave ablation. *J Inflamm Res* 17:4175–4186. <https://doi.org/10.2147/JIR.S462650>
- Han X, Wang R, Xu J et al (2019) In situ thermal ablation of tumors in combination with nano-adjuvant and immune checkpoint blockade to inhibit cancer metastasis and recurrence. *Biomaterials* 224:119490. <https://doi.org/10.1016/j.biomaterials.2019.119490>
- Pan H, Tian Y, Pei S et al (2024) Combination of percutaneous thermal ablation and adoptive Th9 cell transfer therapy against non-small cell lung cancer. *Exp Hematol Oncol* 13:52. <https://doi.org/10.1186/s40164-024-00520-8>
- Sun D, Tan L, Chen Y et al (2024) CXCL5 impedes CD8(+) T cell immunity by upregulating PD-L1 expression in lung cancer via PXN/AKT signaling phosphorylation and neutrophil chemotaxis. *J Exp Clin Cancer Res* 43:202. <https://doi.org/10.1186/s13046-024-03122-8>
- St Paul M, Ohashi PS (2020) The roles of CD8(+) T cell subsets in antitumor immunity. *Trends Cell Biol* 30:695–704. <https://doi.org/10.1016/j.tcb.2020.06.003>
- Prokhnevskaya N, Cardenas MA, Valanparambil RM et al (2023) CD8(+) T cell activation in cancer comprises an initial activation

- phase in lymph nodes followed by effector differentiation within the tumor. *Immunity* 56(107–24):e5. <https://doi.org/10.1016/j.immuni.2022.12.002>
29. Barbooy O, Bercovich A, Li H et al (2024) Modeling T cell temporal response to cancer immunotherapy rationalizes development of combinatorial treatment protocols. *Nat Cancer* 5:742–759. <https://doi.org/10.1038/s43018-024-00734-z>
 30. Liu D, Yan J, Ma F, Wang J, Yan S, He W (2024) Reinvigoration of cytotoxic T lymphocytes in microsatellite instability-high colon adenocarcinoma through lysosomal degradation of PD-L1. *Nat Commun* 15:6922. <https://doi.org/10.1038/s41467-024-51386-7>
 31. Delclaux I, Ventre KS, Jones D, Lund AW (2024) The tumor-draining lymph node as a reservoir for systemic immune surveillance. *Trends Cancer* 10:28–37. <https://doi.org/10.1016/j.trecan.2023.09.006>
 32. Bottcher JP, Reis e Sousa C (2018) The role of type 1 conventional dendritic cells in cancer immunity. *Trends Cancer* 4:784–92. <https://doi.org/10.1016/j.trecan.2018.09.001>
 33. Pasqual G, Chudnovskiy A, Victora GD (2023) Monitoring the interaction between dendritic cells and T cells in vivo with LIP-STIC. *Methods Mol Biol* 2618:71–80. https://doi.org/10.1007/978-1-0716-2938-3_5
 34. Wu S, Jiang H, Fang Z et al (2024) Enhanced abscopal anti-tumor response via a triple combination of thermal ablation, IL-21, and PD-1 inhibition therapy. *Cancer Immunol Immunother* 73:138. <https://doi.org/10.1007/s00262-024-03718-1>
 35. Ma S, Ong LT, Jiang Z et al (2025) Targeting P4HA1 promotes CD8(+) T cell progenitor expansion toward immune memory and systemic anti-tumor immunity. *Cancer Cell* 43(213–31):e9. <https://doi.org/10.1016/j.ccell.2024.12.001>
 36. Yang X, Jin Y, Lin Z et al (2023) Microwave ablation for the treatment of peripheral ground-glass nodule-like lung cancer: long-term results from a multi-center study. *J Cancer Res Ther* 19:1001–1010. https://doi.org/10.4103/jcrt.jcrt_1436_23
 37. He N, Huang H, Wu S et al (2024) Microwave ablation combined with PD-L1 blockade synergistically promotes Cxcl9-mediated antitumor immunity. *Cancer Sci* 115:2196–2208. <https://doi.org/10.1111/cas.16182>
 38. Guo RQ, Peng JZ, Li YM, Li XG (2023) Microwave ablation combined with anti-PD-1/CTLA-4 therapy induces an antitumor immune response to renal cell carcinoma in a murine model. *Cell Cycle* 22:242–254. <https://doi.org/10.1080/15384101.2022.2112007>
 39. Cao B, Liu M, Wang L et al (2022) Remodelling of tumour micro-environment by microwave ablation potentiates immunotherapy of AXL-specific CAR T cells against non-small cell lung cancer. *Nat Commun* 13:6203. <https://doi.org/10.1038/s41467-022-33968-5>
 40. Wang M, Sang J, Xu F et al (2024) Microwave ablation combined with Flt3L provokes tumor-specific memory CD8(+) T cells-mediated antitumor immunity in response to PD-1 blockade. *Adv Sci (Weinh)*. <https://doi.org/10.1002/advs.202413181>
 41. Buchwald ZS, Nasti TH, Lee J et al (2020) Tumor-draining lymph node is important for a robust abscopal effect stimulated by radiotherapy. *J Immunother Cancer*. <https://doi.org/10.1136/jitc-2020-000867>
 42. Mueller SN, Gebhardt T, Carbone FR, Heath WR (2013) Memory T cell subsets, migration patterns, and tissue residence. *Annu Rev Immunol* 31:137–161. <https://doi.org/10.1146/annurev-immunol-032712-095954>
 43. Yang K, Kallies A (2021) Tissue-specific differentiation of CD8(+) resident memory T cells. *Trends Immunol* 42:876–890. <https://doi.org/10.1016/j.it.2021.08.002>
 44. Huang Q, Wu X, Wang Z et al (2022) The primordial differentiation of tumor-specific memory CD8(+) T cells as bona fide responders to PD-1/PD-L1 blockade in draining lymph nodes. *Cell* 185(4049–66):e25. <https://doi.org/10.1016/j.cell.2022.09.020>
 45. Tang X, Mao X, Ling P et al (2024) Glycolysis inhibition induces anti-tumor central memory CD8(+)T cell differentiation upon combination with microwave ablation therapy. *Nat Commun* 15:4665. <https://doi.org/10.1038/s41467-024-49059-6>
 46. Gao T, Yuan S, Liang S, Huang X, Liu J, Gu P, Fu S, Zhang N, Liu Y (2024) In Situ Hydrogel Modulates cDC1-based antigen presentation and cancer stemness to enhance cancer vaccine efficiency. *Adv Sci (Weinh)* 11:e2305832. <https://doi.org/10.1002/advs.202305832>
 47. Peng Q, Qiu X, Zhang Z et al (2020) PD-L1 on dendritic cells attenuates T cell activation and regulates response to immune checkpoint blockade. *Nat Commun* 11:4835. <https://doi.org/10.1038/s41467-020-18570-x>
 48. Pan Y, Xue Q, Yang Y et al (2024) Glycoengineering-based anti-PD-1-iRGD peptide conjugate boosts antitumor efficacy through T cell engagement. *Cell Rep Med* 5:101590. <https://doi.org/10.1016/j.xcrm.2024.101590>

Publisher's Note Springer Nature remains neutral with regard to jurisdictional claims in published maps and institutional affiliations.

Authors and Affiliations

Fengkuo Xu¹ · Jing Sang² · Nan Wang³ · Meixiang Wang¹ · Yahan Huang⁴ · Ji Ma¹ · Huanan Chen^{1,5,6} · Qi Xie^{1,7} · Zhigang Wei^{1,8} · Xin Ye^{1,7} 

✉ Qi Xie
xieqi@sdfmu.edu.cn

✉ Zhigang Wei
weizhigang321321@163.com

✉ Xin Ye
yexintaian2020@163.com

¹ Department of Oncology, Lung Cancer Center, The First Affiliated Hospital of Shandong First Medical University & Shandong Provincial Qianfoshan Hospital, Shandong Lung Cancer Institute, Jinan 250014, China

² Department of Pathology, The Affiliated Taian City Central Hospital of Qingdao University, Taian 271000, Shandong, China

³ Department of First Clinical Medical College, Shandong University of Traditional Chinese Medicine, Shandong Provincial Qianfoshan Hospital, Jinan 250014, Shandong, China

⁴ Jinan Third People's Hospital, Jinan, China

⁵ Department of Health Management, The First Affiliated Hospital of Shandong First Medical University & Shandong

Provincial Qianfoshan Hospital, Shandong. Engineering Laboratory for Health Management, Shandong Medicine and Health Key Laboratory of Laboratory Medicine, Jinan 250014, China

- ⁶ Department of Medical Record Management and Statistics, The First Affiliated Hospital of Shandong First Medical University & Shandong Provincial Qianfoshan Hospital, Jinan 250014, China

- ⁷ Shandong Provincial Lab for Clinical Immunology Translational Medicine in Universities, Jinan 250014, China

- ⁸ Cheeloo College of Medicine, Shandong University, Jinan 250033, China